ЖЭТФ, 2008, том 134, вып. 4 (10), стр. 726–739

PHOTO- AND PRESSURE-INDUCED TRANSFORMATIONS IN THE LINEAR ORTHORHOMBIC POLYMER OF C_{60}

K. P. Meletov [a*], ***V. A. Davydov*** [b], ***J. Arvanitidis*** [c,d], ***D. Christofilos*** [c], ***K. S. Andrikopoulos*** [c], ***G. A. Kourouklis*** [c]

[a] *Institute of Solid State Physics, Russian Academy of Sciences 142432, Chernogolovka, Moscow Region, Russia*

[b] *Institute of High Pressure Physics, Russian Academy of Sciences 42092, Troitsk, Moscow Region, Russia*

[c] *Physics Division, School of Technology, Aristotle University 54124, Thessaloniki, Greece*

[d] *Department of Applied Sciences, Technological Educational Institute of Thessaloniki 57400, Sindos, Greece*

Received April 17, 2008

Stability of the linear orthorhombic polymer of C_{60} under pressure and laser irradiation is studied by Raman scattering and X-ray diffraction measurements. The Raman spectrum at ambient pressure remains unchanged, in the time scale of the experiment, up to the intensity 3200 W/cm^2 of the 514.5 nm line of an Ar^+ laser, but irreversible changes are observed at higher intensities. The Raman spectra recorded at increased pressure show similar irreversible changes even at the laser intensity as low as 470 W/cm^2. The X-ray diffraction and Raman measurements of the pressure-treated samples, performed after pressure release, show that the non-irradiated material does not exhibit any changes in the crystal structure and phonon spectra. This behavior indicates a pressure-enhanced photo-induced transformation to a new polymeric phase characterized by a Raman spectrum that differs from those of the other known polymeric phases of C_{60}. The Raman spectra of the photo-transformed linear orthorhombic polymer of C_{60} were measured at the pressure up to 29 GPa. The pressure dependence of the Raman mode frequencies show singularities near 4 GPa and 15 GPa, respectively related to a reversible phase transition and an irreversible transformation to a metastable disordered phase. The diffuse Raman spectrum of the disordered phase does not exhibit essential changes with an increase in pressure up to 29 GPa. The high-pressure phase transforms to a mixture of pristine and dimerized C_{60}, after pressure release and exposure to ambient conditions for 30 hours.

PACS: 61.48.-c, 62.50.-p, 64.70.K-, 78.30.Na, 78.55.Kz

1. INTRODUCTION

Polymerization of the monomeric FCC (face-centered cubic) phase of C_{60} can be performed by various ways of sample treatment [1–4]. In particular, the polymerization of fullerene C_{60} caused by light illumination from an Ar^+ laser beam at 514.5 nm with a power density exceeding 5 W/cm^2 has been observed [1]. Photo-polymerization is related to covalent bonding between adjacent C_{60} molecules via [2 + 2] cycloaddition reactions that result in the creation of fullerene dimers and/or oligomers $(C_{60})_n$, with n = 2–20 [1, 5–7]. Because of the small light penetration depth ($\sim 1\,\mu$m), the photo-polymerization is effective only in thin films or surfaces of bulk samples, making the X-ray analysis of the photo-polymer structure rather uncertain [8].

In contrast to the photo-polymerization of the FCC phase of C_{60}, products of the high-pressure/high-temperature (HPHT) polymerization, proceeding basically through the [2 + 2] cycloaddition reaction,

*E-mail: mele@issp.ac.ru

are bulk crystalline samples based on various low- and high-molecular mass linear (1D), planar (2D), or cross-linked (3D) polymers of C_{60} with intermolecular covalent bonding via sp^3-like coordinated carbon atoms [3, 4, 9–11]. The structural ordering of the high-molecular-mass polymers gives rise to the formation of crystalline structures that were identified as linear orthorhombic (1D–O), planar tetragonal (2D–T), or rhombohedral (2D–Rh) and face-centered cubic (3D–FCC) depending on the C_{60} coordination within the polymeric network [3, 4, 6, 7, 11].

The formation of dimers, linear polymeric chains, planar polymeric layers, or polymeric networks results in distinct changes in the Raman and IR spectra related to the lowering of the C_{60} molecular symmetry, which leads to the splitting of the bands and their softening due to a decrease in the mean intramolecular bond strength [1–4, 6, 9]. The number of sp^3-like coordinated carbon atoms per C_{60} cage depends on the polymer structure and increases from 4 to 8 and to 12 for 1D–O, 2D–T, and 2D–Rh polymeric phases, respectively. The relatively small number of sp^3-like coordinated carbon atoms in linear and planar polymers of C_{60} leaves open the possibility for their further polymerization, in particular by application of uniaxial pressure perpendicular to the polymeric sheets of the planar and/or to the polymeric chains of linear polymers of C_{60}, as it follows from numerical calculations [12, 13].

According to the calculations in [12], the planar 2D–T polymer transforms into a 3D-polymer with 24 sp^3-like coordinated carbon atoms per C_{60} molecule under a pressure of approximately 20 GPa via covalent bonding between molecules in adjacent polymeric sheets. Another calculation [13] predicted that uniaxial compression of linear and planar polymers of C_{60} leads to 3D polymerization with 52, 56, and even 60 sp^3-like coordinated carbon atoms per C_{60} molecular cage. Experimental *in situ* Raman and X-ray studies of the 2D–T polymer at high pressure have revealed an irreversible transition near 20 GPa to an ordered high-pressure phase, related to its three-dimensional polymerization [14, 15]. The *in situ* Raman study of the 2D–Rh polymer at high pressure has revealed an irreversible transition near 15 GPa to a disordered metastable phase [16], related most likely to random bonding of molecules belonging to adjacent polymeric sheets.

Recently, based on our Raman study of the pressure behavior of the linear 1D–O polymeric phase of C_{60}, we reported an irreversible transformation of the material under laser irradiation and high pressure [17]. The photo-induced transformation occurs even at normal pressure, while the simultaneous application of pressure and laser irradiation drastically increases the transformation rate [18]. Raman spectra of the photo-transformed 1D–O polymer differ from those of the known polymeric phases of C_{60} [17]. Finally, an independent X-ray powder diffraction study has shown that under simultaneous application of pressure and X-ray irradiation, the 1D–O polymer transforms into a new polymeric phase characterized by conjunction of adjacent polymeric chains [19].

In this paper, we report and discuss the results of an extended study of the pressure-enhanced photo-induced polymerization of the 1D–O polymer at room temperature. We investigate the influence of the laser irradiation intensity on the Raman spectra of the 1D–O polymer excited by the 514.5 nm Ar^+ laser line as well as the enhancement of the photo-polymerization rate at high pressure. We also report the detailed study of the pressure behavior of the photo-transformed 1D–O polymer of C_{60} at pressures up to 29 GPa and at room temperature by means of *in situ* Raman scattering. The pressure dependence of the phonon frequencies of the photo-transformed 1D–O polymer revealed a pressure-induced phase transition near 4 GPa and an irreversible transformation at 15 GPa related to its further polymerization.

2. EXPERIMENTAL

Samples of the 1D–O polymeric phase of C_{60} were prepared from sublimed 99.98 % pure C_{60} powder at 1.2 GPa and 573 K in a "toroid"-type device. The preliminary X-ray analysis confirmed that the samples have the well-known orthorhombic packing of linear polymeric chains (space group $Pmnn$: $a = 9.098$ Å, $b = 9.831$ Å, and $c = 14.72$ Å). The specimens used for the high-pressure measurements had dimensions of approximately 100 μm and were selected from the batch material by means of micro-Raman probing for their intense, clear, and spatially uniform Raman spectrum, typical of the 1D–O polymeric phase [9].

Raman spectra were recorded in the backscattering geometry using a micro-Raman system equipped with a triple monochromator (DILOR XY) and a CCD liquid-nitrogen cooled detector system. The spectral width of the system was approximately 3 cm^{-1}. The 514.5 nm line of an Ar^+ laser with the beam intensity in the range 0.005–0.5 mW on the sample was used for excitation. The laser line was focused on the sample by means of 100× and 20× objectives with the respective spatial resolutions around 1 and 2.7 μm. The

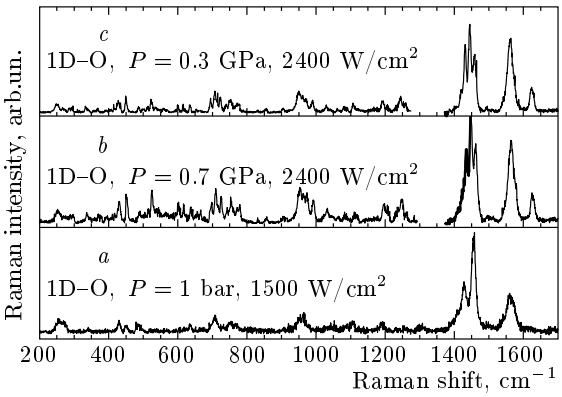

Fig. 1. Raman spectrum of the initial linear orthorhombic polymer of C_{60} at normal conditions (a) and the spectrum of the transformed sample at 0.7 GPa (b). Another specimen shows the same transformation of the Raman spectrum at 0.3 GPa (c)

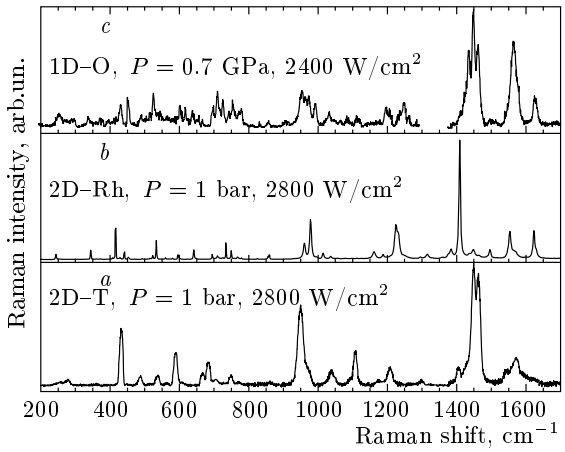

Fig. 2. Raman spectra of the 2D–T (a), 2D–R (b), and the transformed 1D–O (c) polymeric phases of C_{60}

Raman spectra were measured at high pressures using a Mao–Bell-type diamond anvil cell (DAC) [20]. The 4:1 methanol–ethanol mixture was used as a pressure-transmitting medium and the ruby fluorescence technique was used for pressure calibration [21].

3. RESULTS AND DISCUSSION

The Raman spectrum of the pristine 1D–O polymer recorded at ambient conditions is shown in Fig. 1a. This spectrum coincides with the earlier reported spectrum of the 1D–O polymeric phase: the number of the Raman active modes, the peak positions, and their intensities are practically the same within the accuracy of the measurements [9]. Figure 1b shows the Raman spectrum of the 1D–O polymer recorded in the first run of the high-pressure Raman measurements at the starting pressure 0.7 GPa obtained on loading the DAC. The spectrum in Fig. 1b has quite different structure: the majority of the bands are split and the total number of peaks is increased. The same behavior is observed for several experimental runs with different specimens of the 1D–O polymer at any starting pressure after the sample loading into the DAC. We could not find the threshold pressure for this transformation: it occurs even at a pressure as low as 0.1 GPa. Figure 1c demonstrates that the Raman features of the transformed 1D–O polymer are identical for any initially generated pressure.

Figure 2 shows the Raman spectrum of the transformed 1D–O polymer compared with the Raman spectra of the planar 2D–Rh and 2D–T polymeric phases of C_{60}. The comparison of the Raman spectra of the transformed 1D–O polymer (Fig. 2c) to those of the 2D–T (Fig. 2a) and 2D–Rh (Fig. 2b) polymers clearly shows the difference in the number, positions, and relative intensities of the peaks. The increase in the number of peaks testifies that the molecular symmetry of the C_{60} cage in the new phase is lower than in the pristine orthorhombic polymer (symmetry D_{2h}). In the case of the cross-linking of the pristine 1D–O polymer, the lowering of symmetry could be associated with the formation of new inter-cage covalent bonds between the C_{60} clusters that belong to the neighboring polymeric chains in the structure of the orthorhombic phase. The distinction of the Raman spectrum of the transformed 1D–O polymer with respect to those of the 2D polymerized tetragonal and rhombohedral phases of C_{60} indicates that the novel chemical bonds between neighboring polymeric chains of the 1D–O polymer are different from those of the cross-linked polymeric bonds in the planar polymers of C_{60}. The detailed data related to the Raman-mode frequencies of these polymeric phases, as well as the Raman frequencies and the mode assignment of the pristine C_{60} are summarized in Table 1.

To study the structural aspects of the observed transformation, we compared the X-ray diffraction pattern of the initial 1D–O polymer at normal conditions with that of the pressure-treated 1D–O polymer after pressure release. The pressure was increased up to 3 GPa in a "toroid"-type high-pressure cell; the duration of treatment was 10 minutes at 20 °C. The X-ray diffraction pattern of the pristine material at ambient pressure and the pressure-treated 1D–O polymer after the pressure release are shown in Fig. 3. As can be

Table 1. Phonon frequencies for the 2D–Rh, 2D–T, 1D–O, and the transformed 1D–O polymeric phase of C_{60}. The corresponding values for monomeric C_{60} are also included

2D–Rh polymer [22]		2D–T polymer [23]		1D–O transformed [17]		1D–O polymer [17]		Monomeric C_{60} [24]	
Mode[a]	ω_i, cm^{-1}	Mode[b]	ω_i, cm^{-1}	Mode[c]	ω_i, cm^{-1}	Mode[d]	ω_i, cm^{-1}	Mode	ω_i, cm^{-1}
$H_g(1)$	245	$H_g(1)$	259		248	$H_g(1)$	251	$H_g(1)$	273
$H_g(1)$	267		280		266		270		
$H_g(1)$	308				288				
$H_u(1)$	342				333		340		
$F_{2u}(1)$	366				366				
					389				
$G_u(1)$	406								
$H_g(2)$	415				411				
$H_g(2)$	438	$H_g(2)$	431		427	$H_g(2)$	425	$H_g(2)$	437
$H_g(2)$	451						450		
$A_g(1)$	492	$A_g(1)$	481		484	$A_g(1)$	486	$A_g(1)$	496
$F_{1u}(1)$	520				521	$\Omega(x)$	523		
$F_{2g}(1)$	532	$F_{2g}(1)$	536		527				
$F_{1g}(1)$	558	$F_{1g}(1)$	563		561				
$H_u(2)$	579	$F_{1g}(1)$	588						
$H_u(2)$	596				598				
		$\Omega(x)$	610		614				
$H_u(3)$	640				634	$H_g(3)$	635		
					654				
		$H_g(3)$	666		662				
$H_g(3)$	695				694				
$F_{2u}(2)$	709				707		707	$H_g(3)$	710
$H_g(3)$	712				722				
$H_g(3)$	731				739				
$H_g(4)$	749	$H_g(4)$	747		752	$H_g(4)$	752		
$F_{2g}(2)$	767								
$H_g(4)$	776		772		774		769	$H_g(4)$	774
$F_{2u}(3)$	827								
$H_u(4)$	856				853	$\Omega(x)$	843		
$H_u(4)$	868	$\Omega(x)$	864						
					903	$\Omega(x)$	897		

Table 1. (Continued)

2D–Rh polymer [22]		2D–T polymer [23]		1D–O transformed [17]		1D–O polymer [17]		Monomeric C_{60} [24]	
Mode[a]	ω_i, cm^{-1}	Mode[b]	ω_i, cm^{-1}	Mode[c]	ω_i, cm^{-1}	Mode[d]	ω_i, cm^{-1}	Mode	ω_i, cm^{-1}
$G_g(2)$	958	$G_g(2)$	951		947	$\Omega(x)$	957		
					959				
$F_{1g}(2)$	977	$F_{1g}(2)$	970		969				
					987				
$F_{2u}(4)$	1016								
$F_{2u}(4)$	1037				1027	$\Omega(x)$	1034		
$H_g(5)$	1042	$\Omega(x)$	1041						
$H_g(5)$	1078	$H_g(5)$	1090		1082	$H_g(5)$	1082		
$H_g(5)$	1109		1107		1105		1105	$H_g(5)$	1100
$G_g(3)$	1158	$G_g(3)$	1176						
$G_g(3)$	1195				1190		1190		
$F_{2g}(3)$	1204	$F_{2g}(3)$	1206		1205				
$H_g(6)$	1224								
$H_g(6)$	1230				1241	$H_g(6)$	1240	$H_g(6)$	1243
$H_g(6)$	1260				1257		1258		
$G_g(4)$	1314	$G_g(4)$	1299				1307		
$H_g(7)$	1385	$H_g(7)$	1404		1386	$H_g(7)$	1398		
$A_g(2)$	1410				1423		1416		
			1428		1429		1430	$H_g(7)$	1428
		$A_g(2)$	1447		1442		1442		
		$F_{1g}(3)$	1463		1455	$A_g(2)$	1457	$A_g(2)$	1470
$F_{1g}(3)$	1495								
$H_g(8)$	1554	$F_{2g}(4)$	1543		1559				
$H_g(8)$	1563	$H_g(8)$	1567		1559	$H_g(7)$	1560		
$H_g(8)$	1569	$G_g(6)$	1598				1575	$H_g(8)$	1575
$G_g(6)$	1621				1621		1621		
$G_g(6)$	1627								

[a] The peak positions and mode assignment for the 2D–Rh polymeric phase refer to the irreducible representations of the C_{60} molecule and follow Ref. [9] in general.
[b] The mode assignment for the 2D–T polymeric phase follows that in Ref. [9]. The modes marked by $\Omega(x)$ have unclear assignment.
[c] No assignment can be made.
[d] The mode assignment for the 1D–O polymeric phase follows that in Ref. [25].

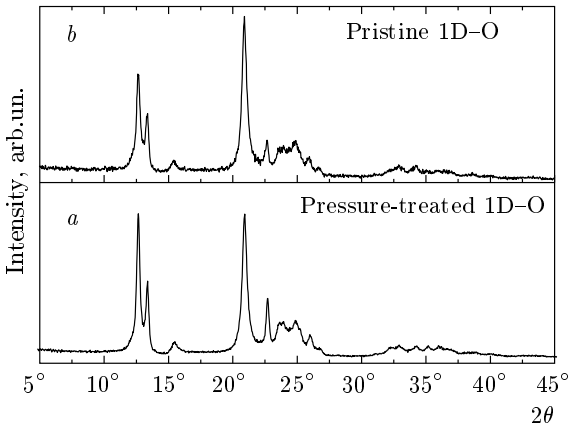

Fig. 3. X-ray diffraction pattern of the pressure-treated 1D–O polymer after pressure release (a) and the initial orthorhombic phase of C_{60} at normal conditions (b)

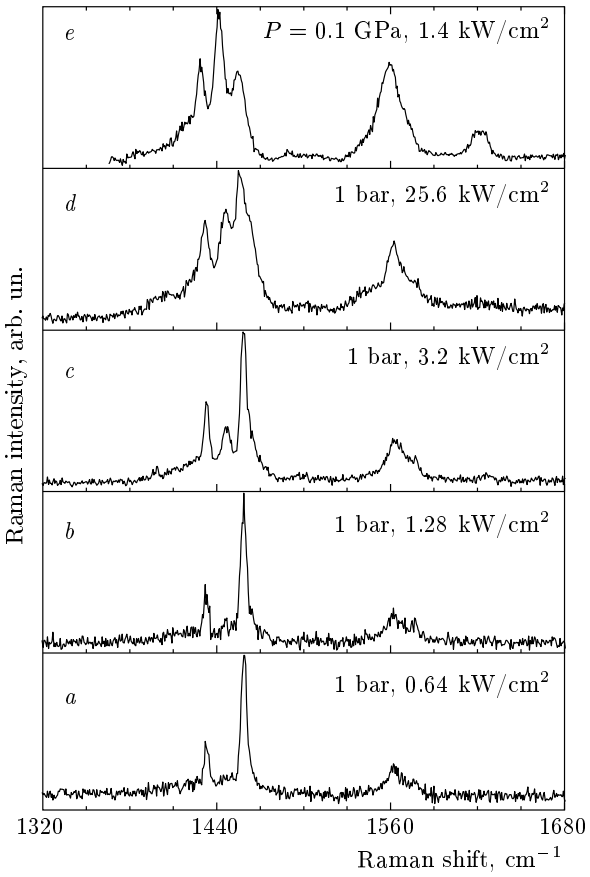

Fig. 4. Raman spectra of the pristine 1D–O polymer recorded at ambient conditions and various excitation intensities of the 514.5 nm Ar^+ laser line (a–d) in comparison with that of the transformed material at 0.1 GPa (e)

from Fig. 3, there are no significant differences in the X-ray diffraction patterns of the 1D–O polymer before and after the pressure treatment. The positions of all observed peaks are the same, while small differences in peak intensities may be related to the powder material preparation. In addition, the *ex situ* Raman spectrum of the pressure-treated 1D–O polymer taken after pressure release is the same as the spectrum of the initial polymer. The fact that the *ex situ* X-ray and Raman data of the high-pressure-treated 1D–O polymer do not show any changes in the crystal structure and the phonon spectrum of the material, contrary to the transformation clearly observed in the *in situ* high-pressure Raman study, implies that the material transformation is related to the combined effect of laser irradiation and high-pressure application. Therefore, the observed transition is related to pressure-enhanced photo-induced polymerization of the material.

It is known that the HPHT 2D and 3D polymers are stable at ambient conditions, and laser irradiation does not cause changes related to their further polymerization. To check the stability of the linear orthorhombic polymer of C_{60} under laser irradiation at ambient conditions, we measured the Raman spectra of the 1D–O polymer at various intensities of the 514.5 nm Ar^+ laser line. The results of these measurements are presented in Fig. 4. The spectrum in Fig. 4a, measured at the laser intensity 640 W/cm^2, is identical to the Raman spectrum of the pristine 1D–O polymer and does not show any traces of a photo-induced transformed phase. The increase in laser intensity to approximately 1280 W/cm^2 (Fig. 4b) does not affect the Raman features within the time scale of the experiment, while a new Raman band appears near 1446 cm^{-1} at the laser intensity 3200 W/cm^2. A further increase in the laser intensity to 6400 W/cm^2 and subsequently to 12800 W/cm^2 leads to a gradual intensity enhancement of the new band (not shown in the figure). At the same time, the two bands near 1433 cm^{-1} and 1563 cm^{-1} become stronger with respect to the main band near 1458 cm^{-1}, which is attributed to the "pentagonal pinch" $A_g(2)$ intramolecular mode of C_{60} in the pristine 1D–O polymer [9]. At the highest laser intensity 25600 W/cm^2 (Fig. 4d), the Raman bands broaden significantly and shift slightly to lower energies due to sample heating, which results in its gradual degradation within the laser beam spot under long time exposure. We note that this spectrum is reminiscent of the Raman spectrum of the photo-transformed 1D–O polymer taken at $P = 0.1$ GPa with the laser intensity 1400 W/cm^2 (Fig. 4e).

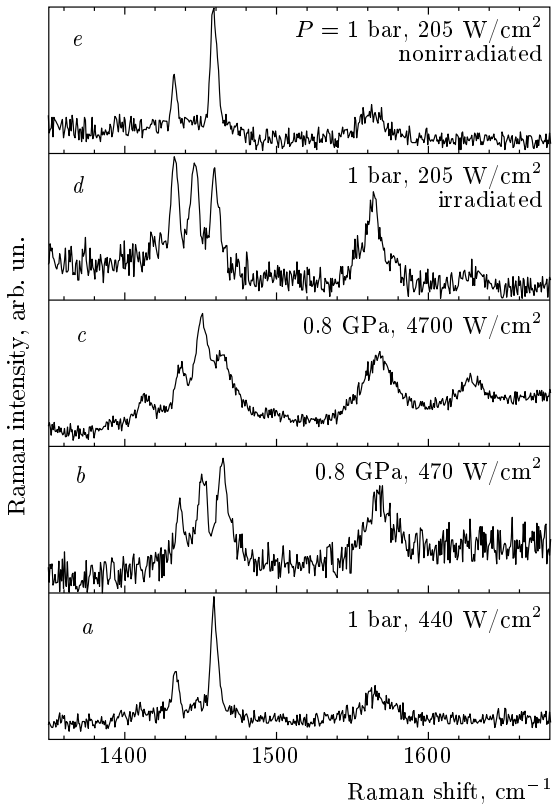

Fig. 5. Raman spectra of the 1D–O polymer recorded at various pressures and excitation intensities of the 514.5 nm Ar^+ laser line. The pressure-assisted photopolymerization starts at the relatively low laser power 470 W/cm^2 (*b*). After pressure release, the laser-treated sites show Raman spectra typical of the photo-polymer (*d*), while untreated sites do not show any photopolymerization effects (*e*)

Figure 5 depicts the Raman spectra of the 1D–O polymer measured at various conditions of laser intensity and pressure. The Raman spectrum of the 1D–O polymer shown in Fig. 5*a* refers to ambient conditions at the laser intensity ~ 440 W/cm^2. Apparently, these experimental conditions do not cause changes related to photopolymerization. At the pressure 0.8 GPa, the changes in the Raman spectrum appear at the laser intensity approximately 470 W/cm^2 (Fig. 5*b*). Further increasing the laser intensity to approximately 4700 W/cm^2 leads to an almost instantaneous transformation of the material to a new phase (Fig. 5*c*). The Raman spectrum recorded in the DAC after pressure release shows the same features as the spectra recorded under the pressure 0.8 GPa (Fig. 5*d*). This indicates that the new phase that appears at the sample sites treated by laser irradiation at high pressure remains stable at ambient conditions. On the contrary, the sample sites that were not irradiated by the laser beam at high pressure show typical Raman features of the pristine 1D–O polymer (Fig. 5*e*). To avoid any influence of laser irradiation on the Raman spectra acquired after pressure release (Fig. 5*d,e*), the measurements were performed at the laser intensity 205 W/cm^2, which is considerably lower than the intensity 3200 W/cm^2 at which the first Raman features related to photopolymerization at ambient pressure appear.

These data imply that the irreversible changes in the Raman spectra of the pristine 1D–O polymer are related to the laser irradiation of the samples, which leads to its further photo-induced polymerization. We note that the photo-induced polymerization of the 1D–O polymer, observed for the first time at ambient conditions for a C_{60} polymer of the HPHT type, occurs at the laser intensity 3200 W/cm^2, a value more than two orders of magnitude greater than the intensity 5 W/cm^2 reported for the photopolymerization of the monomeric C_{60} [1].

The application of high pressure enhances the process, resulting in a drastic increase in the photopolymerization rate and in the subsequent reduction of the laser intensity inducing the transformation. It is important to note that the molecules in the ground state cannot take part in the formation of C_{60} dimers via the [2 + 2] cycloaddition reaction, which is the first step in the polymerization process. According to the Woodward–Hoffmann rule, the straightforward coupling of C_{60} molecules in their ground state is not favorable due to the symmetry of the highest occupied orbital of C_{60} [26, 27]. However, the molecular orbital of the excited state of C_{60}, being populated by light absorption, has a symmetry favorable for dimer formation. On the contrary, the formation of dimers at high pressure occurs even at room temperature without light irradiation [28], which means that the highest occupied molecular orbital of C_{60} at high pressure escapes symmetry limitations on the pair interaction related to the Woodward–Hoffmann rule. In view of this, the simultaneous effect of pressure and light irradiation can stimulate the polymerization process, which results in a considerable increase in the polymerization rate. The results in this work confirm that the 1D–O polymer indeed becomes more sensitive to photochemical reactions when high pressure is applied.

As regards the possible mechanism of the high pressure photo-induced polymerization of the pristine 1D–O polymer, one can speculate that it may be similar to the mechanism of high-pressure photo-induced transformation of other molecular carbon compounds with

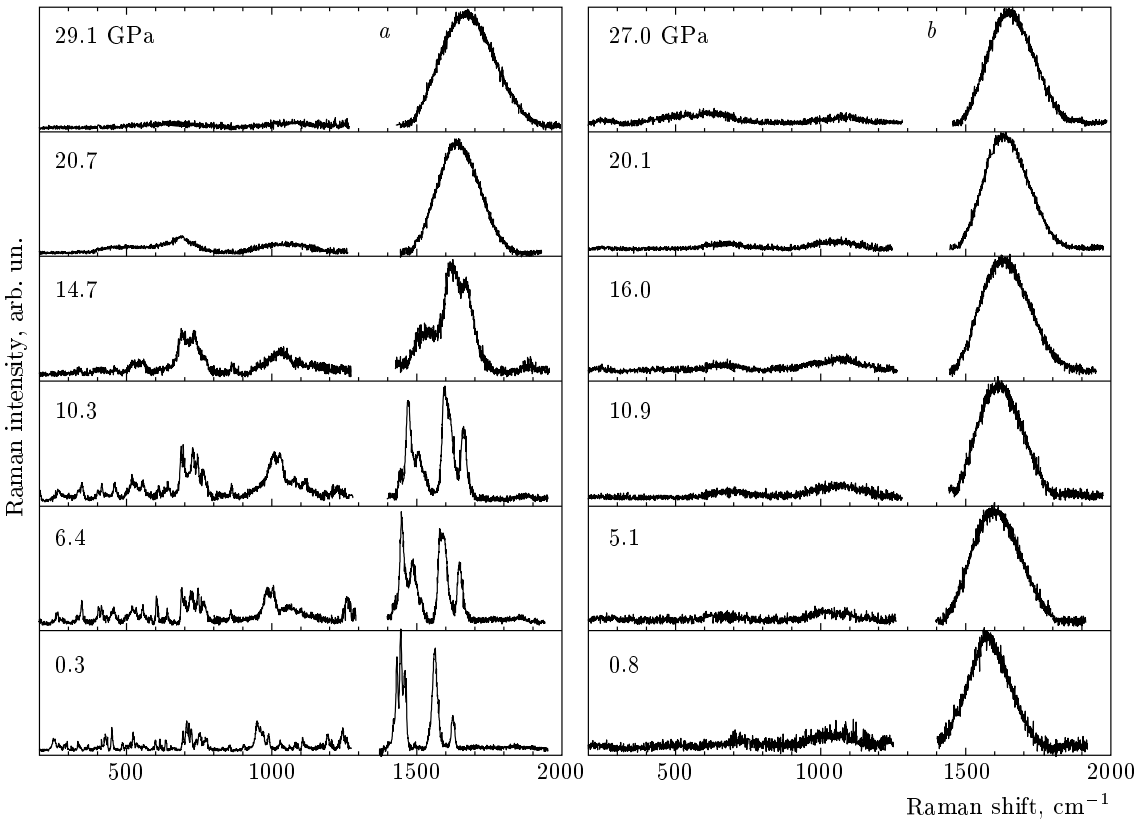

Fig. 6. Raman spectra of the photo-transformed 1D–O polymer of C_{60} at room temperature and various pressures. Spectra recorded upon pressure increase (a), decrease (b)

unsaturated bonds. In particular, the combined action of pressure and laser irradiation reduces the pressure threshold of the chemical transformation of crystalline benzene from 23 to 16 GPa [29]. According to this report, high pressure induces a distortion of the benzene ring that resembles the molecule in the first excited electronic state S_1. The change of molecular geometry relates to the pressure-induced mixing of the excited S_1 state with the S_0 ground state. That is, the distortion of the molecule at high pressure speeds up the photochemical transformation related to the selective pumping of the system in the S_1 excited state.

The structural features of the pressure-enhanced photo-induced polymerization of the 1D–O polymer may be attributed to the bonding between the linear polymeric chains. The lowering of symmetry, indicated by the appearance of new Raman peaks, can be associated with the formation of new covalent bonds between the C_{60} molecules that belong to the neighboring polymeric chains in the structure of the orthorhombic phase. The distinction of the Raman spectrum of the transformed 1D–O polymer from those of the 2D polymerized tetragonal and rhombohedral phases of C_{60} is indicative of novel chemical bonds in the transformed orthorhombic phase that are not the typical [2 + 2] cycloaddition bonds but single bonds between polymeric chains. The *in situ* high-pressure X-ray powder diffraction study has clearly shown that the 1D–O polymer transforms to a new polymeric phase characterized by conjunction of adjacent linear polymeric chains [19]. This study has not revealed the detailed structure of the new polymeric phase because the low-resolution diffraction profiles along with the small number of peaks did not permit further refinement; nevertheless, additional synchrotron radiation X-ray diffraction experiments may clarify this issue.

Subsequently, the pressure behavior and stability of the photo-transformed 1D–O polymer up to 29 GPa was studied by means of Raman measurements. The Raman spectra of the photo-transformed 1D–O polymer of C_{60} at various pressures and room temperature are shown in Fig. 6. Figure 6*a* illustrates data recorded upon pressure increase and Fig. 6*b* illustrates data recorded during pressure release. The spectral

region around the strong triply degenerate T_{2g} mode of diamond, appearing at 1332 cm^{-1} at ambient pressure [30], is excluded. Moreover, the background, which slightly increases with pressure, is subtracted from the spectra for clarity. The initial Raman spectrum of the photo-transformed 1D–O polymer, which consists of a large number of narrow and well-resolved peaks, demonstrates strong pressure dependence. As the pressure increases, the Raman peaks shift to higher energies and their bandwidth gradually increases. The broadening of the Raman bands is further enhanced above 10 GPa due to the solidification of the pressure-transmitting medium. It is known that the methanol–ethanol mixture is fully hydrostatic up to $\sim$ 10 GPa, while in its glassy form at higher pressures, it supports pressure gradients up to 0.4 GPa [31], which generate shear stress components. The most important pressure effects are related to the changes in the number of the Raman active modes, their pressure coefficients, and intensities. The relative intensities of the Raman modes in the 700–1100 cm^{-1} region gradually increase with respect to other modes. Significant changes were observed near 15 GPa, where the Raman spectrum loses its fine structure in all frequency regions and becomes very diffuse. This transformation was preceded by a rapid decrease in the intensity of the peaks related to the $A_g(2)$ "pentagonal-pinch" (PP) mode of the pristine C_{60} and a relative increase in the intensities of the $H_g(8)$ and $G_g(6)$ modes. The broad Raman features in the spectrum of the high-pressure phase above 15 GPa can be tracked back to the photo-transformed 1D–O polymer of C_{60} and seem to incorporate the corresponding group of the broad Raman bands of this phase.

Despite the similarities in the diffused Raman bands, the spectrum of the high-pressure phase differs significantly from that of the amorphous carbon with respect to the number of peaks as well as to their position. Comparing the Raman spectrum of the high-pressure phase to that of the high-pressure phase of the 2D–T polymeric phase of C_{60} [14, 32], we observe that the former does not contain peaks in the high-energy region, like the 1840 cm^{-1} peak observed in the latter phase. In addition, the new phase shows a spatially uniform Raman response over all the surface of the sample, as was documented by probing various places in the sample, a behavior that differs drastically from the behavior of the 2D–T polymeric phase of C_{60} [14]. We note that the broad Raman features of the high-pressure phase in the photo-transformed 1D–O polymer of C_{60} resemble the Raman features of the disordered high-pressure phase in the 2D–Rh polymer, which was also observed above 15 GPa [16]. Upon pressure decrease, the broad Raman bands of the disordered phase shift to lower energies without any observable changes in their intensity distribution (Fig. 6*b*). After a total release of pressure, the high-pressure phase is rather stable and does not change at least for some hours at normal conditions.

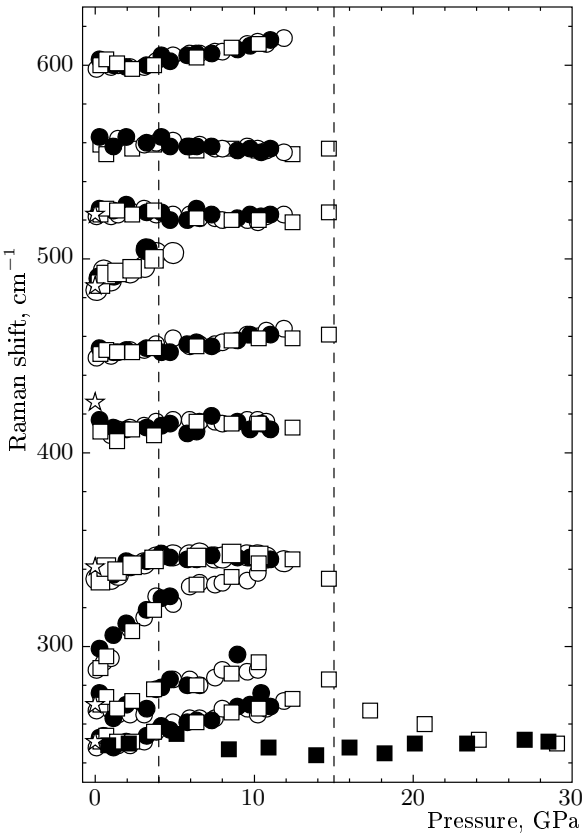

Fig. 7. Pressure dependence of the Raman frequencies of the photo-transformed 1D–O polymer of C_{60} in the range 230–630 cm^{-1}. Circles and squares respectively represent data taken upon two different pressure runs up to 12 GPa and 29 GPa. Stars denote the Raman frequencies of the initial 1D–O polymer at normal conditions. The open (solid) symbols represent data recorded upon pressure increase (decrease). Dashed vertical lines near 4 GPa and 15 GPa mark pressure values where changes are observed

The pressure dependence of the Raman mode frequencies of the photo-transformed 1D–O polymer of C_{60} in the energy regions 230–630 cm^{-1}, 625–1100 cm^{-1}, and 1380–1690 cm^{-1} are shown in Figs. 7, 8, and 9. The phonon frequencies were obtained by fitting Voigt peak functions to the experimental data after the background subtraction. In the high-pressure phase, the frequencies were defined with

Table 2. Pressure coefficients of the Raman modes of the transformed 1D–O polymer of C_{60}

ω_i, cm^{-1}	$d\omega_i/dP$, cm^{-1}/GPa		
$P = 1$ bar	$0 < P < 15$ GPa	$0 < P < 4$ GPa	$4 < P < 15$ GPa
248	2.1		
266	2.5		
288		8.4	2.2
333		2.66	0.04
411	0.34		
451	0.85		
484		3.9	
527	−0.38		
561	−0.41		
598	1.31		
634	0.55		
694	−0.67		
707	−0.64		
722	−0.38		
739	−1.1		
752	−0.81		
774	−0.61		
853	0.85		
959	4.4		
969	5.37		
1027	4.72		
1386	6.1		
1407	6.3		
1429		3.2	6.2
1442		7.0	4.0
1455	4.8		
1494	3.7		
1559		4.5	4.9
1559		4.5	4.0
1621	3.6		

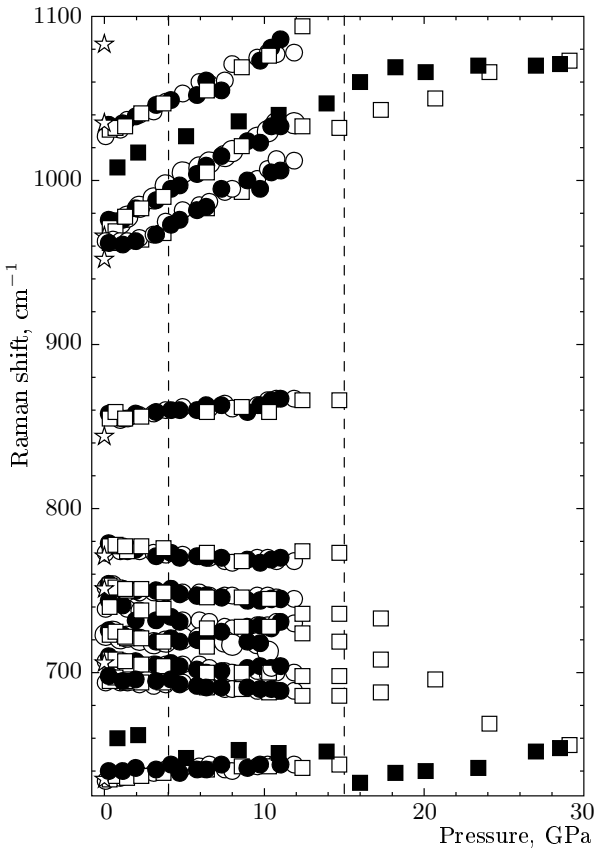

Fig. 8. Pressure dependence of the Raman frequencies of the photo-transformed 1D–O polymer of C_{60} in the range 625–1100 cm^{-1}. Circles and squares respectively represent data taken upon two different pressure runs up to 12 GPa and 29 GPa. Stars denote the Raman frequencies of the initial 1D–O polymer at normal conditions. The open (solid) symbols represent data recorded upon pressure increase (decrease). Dashed vertical lines near 4 GPa and 15 GPa mark pressure values where changes are observed

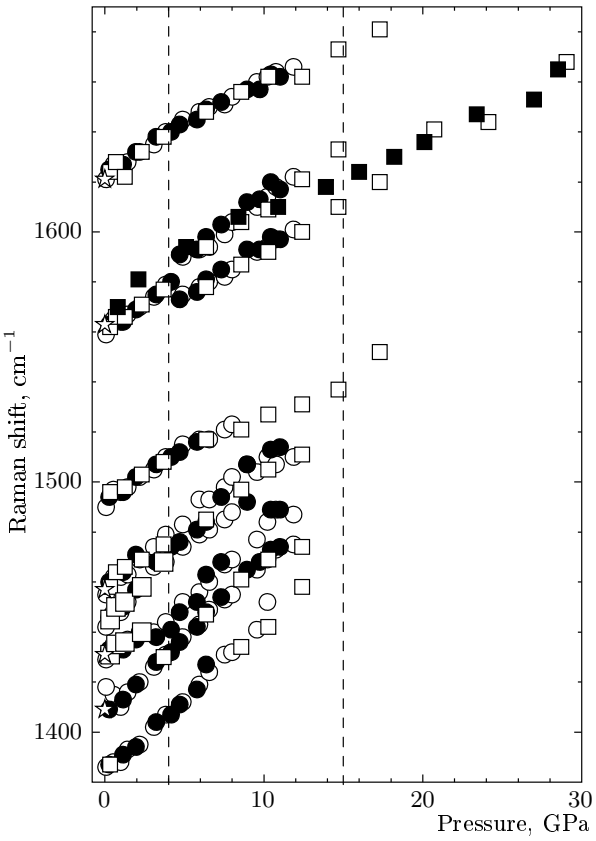

Fig. 9. Pressure dependence of the Raman frequencies of the photo-transformed 1D–O polymer of C_{60} in the range 1380–1690 cm^{-1}. Circles and squares respectively represent data taken upon two different pressure runs up to 12 GPa and 29 GPa. Stars denote the Raman frequencies of the initial 1D–O polymer at normal conditions. The open (solid) symbols represent data recorded upon pressure increase (decrease). Dashed vertical lines near 4 GPa and 15 GPa mark pressure values where changes are observed

a somewhat lower accuracy because of their diffuse nature. Circles and squares represent data taken upon two different pressure runs up to 12 GPa and 29 GPa, respectively. Stars denote the Raman frequencies of the pristine 1D–O polymer at normal conditions. The open (solid) symbols represent data recorded upon pressure increase (decrease). The phonon frequencies obtained upon pressure increase coincide in the two different pressure runs within the accuracy of measurements. The pressure-induced shift of the majority of Raman modes is linear and positive, except for a few modes that display small negative pressure shifts. The pressure coefficients are tabulated in Table 2; their values vary between -0.4 cm^{-1}/GPa (the peak located at 561 cm^{-1}) and $+7.0$ cm^{-1}/GPa (the peak located at 1442 cm^{-1}). The pressure dependence of all Raman modes is reversible with pressure at least up to 12 GPa, the highest pressure reached during the first pressure run. The dashed lines near 4 GPa and 15 GPa indicate the pressure range where changes in the pressure dependence of the Raman peaks occur. The pressure coefficients and the number of Raman bands change abruptly at $\sim$ 4 GPa. The slopes of the low-energy Raman modes at 288 cm^{-1} and 333 cm^{-1} respectively change from 8.4 cm^{-1}/GPa to 2.2 cm^{-1}/GPa and from 2.7 cm^{-1}/GPa to 0.04 cm^{-1}/GPa. For the high-frequency modes at 1429 cm^{-1} and 1442 cm^{-1}, the respective pressure co-

efficients change from 3.2 cm^{-1}/GPa to 6.2 cm^{-1}/GPa and from 7.0 cm^{-1}/GPa to 4.0 cm^{-1}/GPa. In addition, the band at 1559 cm^{-1} splits near 4 GPa and the pressure coefficients of the split components are slightly different; specifically, they are equal to 4.9 cm^{-1}/GPa and 4.5 cm^{-1}/GPa for the higher and the lower-energy component, respectively. The splitting of the mode at 1559 cm^{-1} and the changes in the pressure slopes of a number of modes, along with the reversibility of these effects upon pressure release after reaching 12 GPa, are an indication of a reversible structural phase transition that occurs near 4 GPa. The changes occurring near 15 GPa are apparently related to an irreversible transformation. More specifically, the disappearance of the majority of the phonon modes, the changes in the pressure slopes, the drastic broadening of the Raman bands, and the irreversible behavior upon pressure release are clear evidence of an irreversible transformation to a highly disordered state.

The recovered sample, after pressure release, was tested by means of micro-Raman probing in order to check its stability. Figure 10 shows the Raman spectra of various phases of the 1D–O polymer of C_{60} in the frequency range 1350–1780 cm^{-1}, where the changes in the Raman response are more pronounced. The Raman spectrum of the photo-transformed 1D–O polymeric phase shown in Fig. 10*a* differs significantly from that of the pristine 1D–O polymer shown in Fig. 10*e*. The Raman spectrum of the high-pressure phase of the photo-transformed 1D–O polymer immediately after pressure release is shown in Fig. 10*b*, whereas Figs. 10*c,d* show the Raman spectra of the high-pressure phase at different sites of the sample approximately 30 hours after pressure release. These spectra indicate that the high-pressure phase is metastable and transforms rather quickly to a phase that demonstrates Raman features resembling those of the initial 1D–O polymer of C_{60} (Fig. 10*d*). Nevertheless, the spectrum in Fig. 10*d* is characteristic of a mixture of pristine (monomeric) and dimeric C_{60}, as follows from the position of the $A_g(2)$ PP-mode that is shifted to higher energy than in the initial 1D–O polymer. Noticeably, this behavior is similar to that also exhibited by the 2D–T polymeric phase of C_{60} [14, 32, 33]. The transformation of the recovered 1D–O material was observed at normal conditions without any special heat treatment of the sample except that due to the excitation beam during the Raman probing [34]. The behavior of the recovered high-pressure phase of the photo-transformed 1D–O polymer differs from the behavior of the high-pressure phase of the 2D–Rh polymer, which is more stable and transforms into a mixture of pristine and dimerized C_{60} only after sample annealing at $T > 350\,^{\circ}C$ [16].

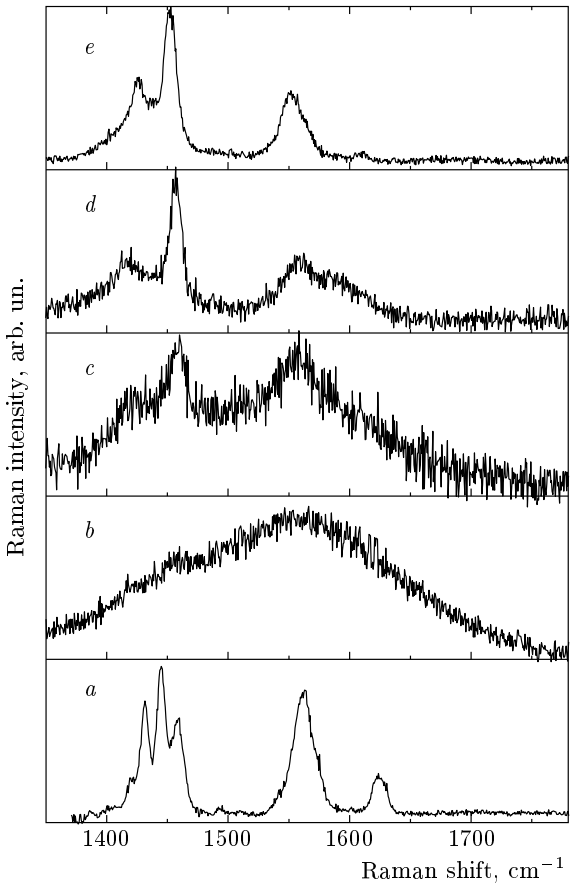

Fig. 10. Raman spectra of various phases of the 1D–O linear orthorhombic polymer of C_{60} in the frequency range 1350–1780 cm^{-1} recorded at normal conditions. *a* — The photo-transformed 1D–O polymeric phase. *b* — The recovered high-pressure phase immediately after pressure release. *c,d* — The Raman spectra of the recovered high-pressure phase at different sites of the specimen recorded approximately 30 hours after pressure release. *e* — The Raman spectrum of the pristine 1D–O polymer

The changes in the pressure dependence of the Raman frequencies of the photo-transformed 1D–O polymer of C_{60} near 4 GPa may be considered an indication of a possible structural phase transition. This may be related to minor changes in the packing of the linked linear polymeric chains. However, to verify that the singularities observed in the high-pressure Raman study are associated with a phase transition, an X-ray study of the structural aspects is necessary. A recent high-pressure X-ray powder diffraction study of the linear orthorhombic polymer of C_{60} has not revealed clear

changes in the diffraction patterns near 4 GPa [19]. However, this study is not yet conclusive because the low resolution of the data and the small number of peaks did not permit the complete refinement of the structure.

The irreversible changes at approximately 15 GPa, from the well-resolved Raman spectrum of the photo-transformed 1D–O polymer to a diffuse one, is typical of a transition to a disordered phase. A rapid decrease in the $A_g(2)$ PP-mode intensity and the enhancement of the neighboring $H_g(8)$ and $G_g(6)$ modes in the pre-transitional pressure regime are reminiscent of the analogous behavior exhibited by these modes in the 2D–T and 2D–Rh polymeric phases of C_{60} before their further polymerization under high pressure [14, 16]. Taking into account that the PP-mode is associated with the in-phase stretching vibrations of the C=C bonds, the decrease in its intensity may be related to the destruction of a number of these bonds and the subsequent creation of covalent links between molecules belonging to adjacent polymeric planes or chains.

Although pressure preferentially decreases the distance between the linear polymeric chains rather than the intercage distance within a chain, the bond formation between the chains is not always preferable. Namely, the C_{60} molecular cages belonging to adjacent polymeric chains may not have optimal relative orientations for the formation of new covalent bonds. Therefore, we expect that the new bonds are formed in a random way due to some distortion in the molecular orientations after photopolymerization. As a result, the new high-pressure phase exhibits a high degree of disorder characterized by a random polymerization. Similarly, in the case of the 2D–Rh polymer, the diffuse Raman spectrum of the high-pressure phase is also related to a disordered polymeric phase of C_{60} characterized by random covalent bonding between molecules belonging to adjacent 2D-polymeric planes of the initial rhombohedral phase. We note that this behavior differs significantly from that of the 2D–T polymeric phase of C_{60}, in which the pressure-induced shortening of the intermolecular distances, accompanied by the optimal orientation of molecules, leads to a high degree of regularity in the formation of the out-of-plane covalent bonds.

In conclusion, the linear orthorhombic polymer of C_{60} is not stable under laser irradiation and transforms into a new polymeric phase. The laser intensity necessary for the photo-induced polymerization at ambient conditions is considerably higher than that needed for the C_{60} monomer. The application of high pressure drastically increases the photopolymerization rate and the transformation becomes almost instantaneous. The *ex situ* X-ray diffraction and Raman studies of the pressure-treated samples performed after pressure release indicate that the nonirradiated material does not exhibit any changes in the crystal structure and the phonon spectrum. This behavior is indicative of a pressure-enhanced photo-induced transformation into a new polymeric phase, which shows different Raman spectrum from those of the known polymeric phases of C_{60}. The *in situ* high-pressure X-ray powder diffraction study shows that the new polymeric phase is characterized by conjunction of the adjacent linear polymeric chains. The high-pressure Raman study of the photo-transformed 1D–O polymer of C_{60} shows a possible structural phase transition near 4 GPa, whereas a further increase in pressure to 15 GPa causes a transformation to a metastable phase with a diffuse spectrum typical of a disordered phase. After pressure release, this phase relaxes to a mixture of pristine and dimerized C_{60}. We assume that this high-pressure phase is formed by the random creation of covalent bonds between linked polymeric chains due to some distortion in the molecular orientation. This assumption is supported by the retention of the fullerene molecular cage in the high-pressure phase and by the similarity in the pretransitional behavior with that of the 2D–T and the 2D–Rh polymeric phases of C_{60}.

The support by the RFBR (grant № 08-02-00890), is greatly acknowledged. K. P. M. acknowledges the support by the General Secretariat for Research and Technology and the hospitality of the Aristotle University of Thessaloniki, Greece.

REFERENCES

1. A. M. Rao, P. Zhou, K.-A. Wang, G. T. Hager, J. M. Holden, Y. Wang, W.-T. Lee, X.-X. Bi, P. C. Eklund, D. S. Cornett, M. A. Duncan, and I. J. Amster, Science **259**, 955 (1993).

2. B. Burger, J. Winter, and H. Kuzmany, Z. Phys. B **101**, 227 (1996).

3. Y. Iwasa, T. Arima, R. M. Fleming, T. Siegrist, O. Zhou, R. C. Haddon, L. J. Rothberg, K. B. Lyons, H. L. Carter Jr., A. F. Hebard, R. Tycko, G. Dabbagh, J. J. Krajewski, G. A. Thomas, and T. Yagi, Science **264**, 1570 (1994).

4. M. Nunez-Regueiro, L. Marques, J.-L. Hodeau, O. Bethoux, and M. Perroux, Phys. Rev. Lett. **74**, 278 (1995).

5. P. C. Eklund, A. M. Rao, P. Zhou, Y. Wang, and J. M. Holden, Thin Solid Films **257**, 185 (1995).

6. M. Sakai, M. Ichida, and A. Nakamura, Chem. Phys. Lett. **335**, 559 (2001).

7. E. Kovats, G. Oszlanyi, and S. Pekker, J. Phys. Chem. B **109**, 11913 (2005).

8. T. Puzstai, G. Oszlanyi, G. Faigel, K. Kamaras, L. Granasy, and S. Pekker, Sol. St. Comm. **111**, 595 (1999).

9. V. A. Davydov, L. S. Kashevarova, A. V. Rakhmanina, V. M. Senyavin, R. Ceolin, H. Szwarc, H. Allouchi, and V. Agafonov, Phys. Rev. B **61**, 11936 (2000).

10. V. D. Blank, S. G. Buga, G. A. Dubitsky, N. R. Serebryanaya, M. Yu. Popov, and B. Sundqvist, Carbon **36**, 319 (1998).

11. V. V. Brazhkin, A. G. Lyapin, S. V. Popova et al., Pis'ma v Zh. Eksp. Teor. Fiz. **76**, 805 (2002).

12. S. Okada, S. Saito, and A. Oshiyama, Phys. Rev. Lett. **83**, 1986 (1999).

13. E. Burgos, E. Halac, R. Weht, H. Bonadeo, E. Artacho, and P. Ordejon, Phys. Rev. Lett. **85**, 2328 (2000).

14. K. P. Meletov, S. Assimopoulos, I. Tsilika, G. A. Kourouklis, J. Arvanitidis, S. Ves, B. Sundqvist, and T. Wägberg, Chem. Phys. Lett. **341**, 435 (2001).

15. D. H. Chi, Y. Iwasa, T. Takano, T. Watanuki, Y. Ohishi, and S. Yamanaka, Phys. Rev. B **68**, 153402 (2003).

16. K. P. Meletov, J. Arvanitidis, G. A. Kourouklis, Y. Iwasa, and K. Prassides, Chem. Phys. Lett. **75**, 406 (2002).

17. K. P. Meletov, V. A. Davydov, A. V. Rakhmanina, V. Agafonov, and G. A. Kourouklis, Chem. Phys. Lett. **416**, 220 (2005).

18. K. P. Meletov, V. A. Davydov, A. V. Rakhmanina, V. Agafonov, J. Arvanitidis, D. Christofilos, K. S. Andrikopoulos, and G. A. Kourouklis, Chem. Phys. Lett. **428**, 298 (2006).

19. R. Le Parc, C. Levelut, J. Haines, V. A. Davydov, A. V. Rakhmanina, R. J. Papoular, E. E. Belova, L. A. Chernozatonskii, H. Allouchi, and V. Agafonov, Chem. Phys. Lett. **438**, 63 (2007).

20. A. Jayaraman, Rev. Sci. Instr. **57**, 1013 (1986).

21. D. Barnett, S. Block, and G. J. Piermarini, Rev. Sci. Instr. **44**, 1 (1973).

22. K. P. Meletov, J. Arvanitidis, G. A. Kourouklis, Y. Iwasa, and K. Prassides, Chem. Phys. Lett. **357**, 307 (2002).

23. J. Arvanitidis, K. P. Meletov, K. Papagelis, S. Ves, G. A. Kourouklis, A. Soldatov, and K. Prassides, J. Chem. Phys. **114**, 9099 (2001).

24. D. S. Bethune, G. Meijer, W. C. Tang, H. J. Rosen, W. G. Golden, H. Seki, C. A. Brown, and M. S. de Vries, Chem. Phys. Lett. **179**, 181 (1991).

25. J. Winter, H. Kuzmany, A. Soldatov, P.-A. Persson, P. Jacobsson, and B. Sundqvist, Phys. Rev. B **54**, 17486 (1996).

26. J. Fagerstrom and S. Stafstrom, Phys. Rev. B **53**, 13150 (1996).

27. E. A. Halevi, Helvetica Chim. Acta **84**, 1661 (2001).

28. V. A. Davydov, L. S. Kashevarova, A. V. Rakhmanina, V. Agafonov, R. Ceolin, and H. Szwarc, Pis'ma v Zh. Eksp. Teor. Fiz. **68**, 881 (1998).

29. L. Ciabini, M. Santoro, R. Bini, and V. Schettino, Phys. Rev. Lett. **88**, 085505 (2002).

30. S. A. Solin and A. K. Ramdas, Phys. Rev. B **1**, 1687 (1970).

31. G. J. Piermarini, S. Block, and J. D. Barnett, J. Appl. Phys. **44**, 5377 (1973).

32. K. P. Meletov, J. Arvanitidis, I. Tsilika, S. Assimopoulos, G. A. Kourouklis, S. Ves, A. Soldatov, and K. Prassides, Phys. Rev. B **63**, 054106 (2001).

33. B. Sundqvist, Adv. Phys. **48**, 1 (1999).

34. K. P. Meletov, E. Liarokapis, J. Arvanitidis, K. Papagelis, G. A. Kourouklis, and S. Ves, Chem. Phys. Lett. **290**, 125 (1998).